



Characterization of products from hydrothermal treatments of cellulose

Ying Gao, Xian-Hua Wang*, Hai-Ping Yang, Han-Ping Chen

State Key Laboratory of Coal Combustion, Huazhong University of Science and Technology, 1037 Luoyu Road, Wuhan, Hubei 430074, PR China

ARTICLE INFO

Article history:

Received 4 December 2011

Received in revised form

9 February 2012

Accepted 12 March 2012

Available online 12 April 2012

Keywords:

Cellulose

Hydrothermal

Bio-oil

Solid residue

ABSTRACT

The main aim of the present study was to investigate the characteristics of products from hydrothermal treatments of cellulose in an autoclave at various temperatures (200 °C–400 °C) and residence times (5 min–2 h). The gas products mainly consisted of CO₂, CO, CH₄, and H₂ at 250 °C–400 °C for 30 min. Heavy oil mainly contained furans, phenols, carboxylic acids, aldehydes, ketones, and high molecular compounds at all hydrothermal temperatures. Aldehydes, phenols, ketones, acid groups and sugars were determined in the aqueous phase by gas chromatography-mass spectrometry and Fourier transform infrared (FTIR). The solid residues were analyzed by elemental analysis, scanning electron microscopy, transmission electron microscopy, x-ray photoelectron microscopy, FTIR, and thermogravimetric analysis techniques. The results showed that the residues had core-shell structure and better physicochemical characterization at lower temperature (250 °C) and longer residence time (2 h).

© 2012 Elsevier Ltd. All rights reserved.

1. Introduction

Renewable energy has generated much interest due to the energy crisis, the rising oil prices, the green house effect, and political factors. Biomass energy is an important energy for sustaining human life, second only to coal, petroleum, and natural gas. Biomass energy ranks fourth in the general energy-consuming quantity of the world; thus, it holds an important position in the international energy system. Biomass energy will be main component in future sustainable energy systems.

Biomass resources, as components of renewable energy, include straws, wood, poultry manures, urban solid waste, and so on. The main components of lignocellulosic biomass are cellulose, hemicellulose, and lignin. Compared with hemicellulose and lignin, cellulose is an important component in biomass, accounting for 40%–50%. Many studies have been reported about the cellulose thermo-chemical process with its simple structure and stable chemical property [1,2]. The conversion processes of cellulose are classified as biochemical conversion (fermentation and digestion) and thermo-chemical conversion (gasification, pyrolysis and hydrothermal treatment) [3–5].

Hydrothermal conversion process is the technique of biomass conversion in sub- or super-critical water under high temperature and pressure without oxygen, also called wet pyrolysis [6]. Hydrothermal processing can be divided into three main stages,

namely, carbonization, liquefaction, and high temperature gasification, which depend on processing temperature and residence time [7]. The properties of target products are mainly determined by the experimental parameters selected.

Kruse et al. studied the super-critical water gasification of cellulose. Their experimental results showed that cellulose rapidly degrades, the hydrogen yield increases and carbon monoxide yield decreases [8]. Donovan et al. observed that reaction conditions affect cellulose hydrothermal liquefaction. Their experimental results showed that oil has large molecular weight and contains more phenolic constituents. The effect of temperature on hydrothermal process and product distribution of biomass is significant [9]. Minowa et al. studied the liquefaction behavior of cellulose at 200 °C–350 °C temperature. They found that cellulose begins to decompose at 200 °C. When the temperature reaches 240 °C–270 °C, the reaction rate is obviously faster than that at lower temperature. The reaction is completed at 280 °C [10,11]. Some researchers reported that heavy oil (HO) yield is higher from the liquefaction of biomass at 300 °C [12,13]. Residence time also affects the hydrothermal liquefaction of biomass. Elliott et al. analyzed the HO from high-moisture biomass and set a residence time of 30 min in their experiment [14]. The results of Zhang et al. showed that the residence time of 10 min is more favorable in producing HO than 30 min under their experimental conditions [15]. However, prolonged residence time does not promote the production of HO; instead, it could raise the yield of bio-char and the formation of organic acid [16]. Sevilla and Fuertes obtained carbonaceous materials from cellulose by hydrothermal carbonization [17]. However, there have been very few studies about the

* Corresponding author. Tel.: +86 27 87542417x8211; fax: +86 27 87545526.

E-mail addresses: gstshwgy@163.com (Y. Gao), wxxwhhy@sina.com (X.-H. Wang), yhpjng2002@163.com (H.-P. Yang), hp.chen@163.com (H.-P. Chen).

properties of target products (gas, HO, aqueous phase, and solid residue (SR)) from cellulose in sub- and super-critical water.

The present paper studied the effect of hydrothermal temperature and residence time on product distribution and characterization. Simultaneously, the physicochemical properties of the target products (gas, HO, aqueous phase, and SR) were analyzed. The investigation focused on the analysis of the liquid products to observe the formation of key compounds using an effective separation procedure from different temperatures.

2. Material and method

2.1. Samples

The microcrystalline cellulose obtained from Wuhan Shenshi Chemical Co., Ltd. was dried at 105 °C until the weight was constant. The main characteristics of the cellulose (wt% of dry basis) are shown in Table 1. The laboratory-grade acetone and ether were purchased from Wuhan Shenshi Chemical Co., Ltd.

2.2. Apparatus and procedure

All experiments were carried out in a 500 ml autoclave of 316L stainless steel. The autoclave can be operated at a maximum temperature of 600 °C and maximum pressure of 40 MPa. The autoclave was heated by electrical heater. The temperature was measured with a thermocoupler and controlled at ± 5 °C. The pressure was measured at an accuracy of 2%.

For each test, 8 g of the cellulose and 110 g of the deionized water were placed in the autoclave and sealed. The reactor was purged and pressurized to 2 MPa using argon. Then, the experimental setup was heated from ambient temperature to 200 °C–400 °C. The retention time was 5 min to 2 h. All experiments were repeated three times and averaged using a set of numbers.

All experiments followed the same temperature profile (Fig. 1). Cool-down at the end of each experiment was achieved by internal cooling U-loop and external fan. Reactor temperature fell below 90 °C in less than 15 min for each experiment. The gas was collected by gas bag for further analysis. When the temperature dropped to room temperature, the remaining gas was vented. The autoclave solid–liquid mixture were collected and separated. With the filter device, the water-soluble fraction was taken as aqueous phase and centrifuged at 4000 rpm to remove the suspended solids. The filtered water solution was evaporated at 75 °C under atmospheric pressure to completely remove the water before Fourier transform infrared (FTIR) for identifying the sugar products. Part of filtered water solution was extracted by laboratory-grade ether at 25 °C in a rotary evaporator at atmospheric pressure, and the residue liquids were analyzed by gas chromatography–mass spectroscopy (GC–MS) for identifying sugar-derived compounds. The water-insoluble fractions, retained on the autoclave and stirring blade were washed three times with laboratory-grade acetone. The

Table 1
Main characteristics of the cellulose.

Characteristics	Cellulose
Elemental analysis ^a (%)	
Carbon	42.93
Hydrogen	9.06
Nitrogen	0.0045
Oxygen ^b	43.69
Empirical formula	CH _{2.53} O _{0.76}
H/C molar ratio	2.53
O/C molar ratio	0.83

^a Weight percentage on dry ash free basis.

^b By difference.

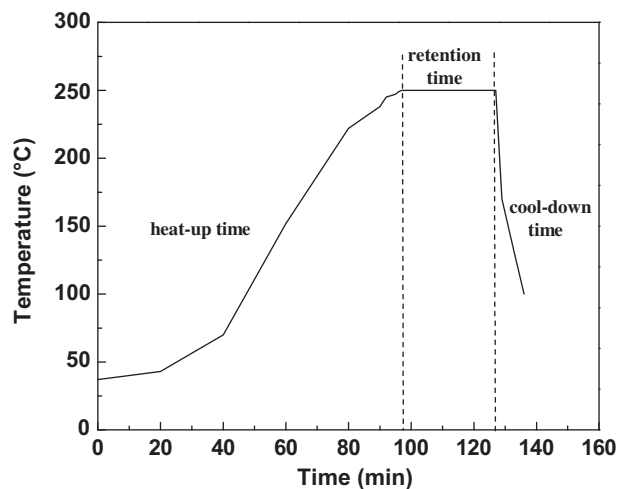


Fig. 1. Schematic diagram of a typical temperature cycle for 500 mL autoclave reactor to 250 °C with 30 min retention time.

acetone soluble fraction and insoluble fraction were separated by filtration. Finally, the acetone solution was dried at 45 °C in the rotary evaporator at 0.006 MPa, and the residue was weighed and designated as HO. The solid insoluble in acetone was dried at 105 °C to obtain the SR. The procedure for separating products is shown in Fig. 2. The yields of the HO and SR were defined as weight percentage to the raw material.

$$\text{HO Yield (wt. \%)} = (\text{weight of HO}) / (\text{weight of raw material}) \times 100\%$$

$$\text{SR Yield (wt. \%)} = (\text{weight of SR}) / (\text{weight of raw material}) \times 100\%$$

2.3. Analysis of gas

Micro-GC: The gas products were analyzed by a Four-Channels Micro-Gas Chromatograph (Micro-GC, Agilent 3000). The three columns used were as follows: (1) Column A (molecular sieve) for analysis of H₂, O₂, N₂, CH₄, and CO at 95 °C; (2) Column B (Plot U) for analysis of CO₂ and some hydrocarbons (C₂H₄, C₂H₂, and C₂H₆) at 100 °C; (3) Column C (aluminum oxide) for analysis of C₃H₈ and C₃H₆ at 140 °C. The carrier gas was high-purity helium.

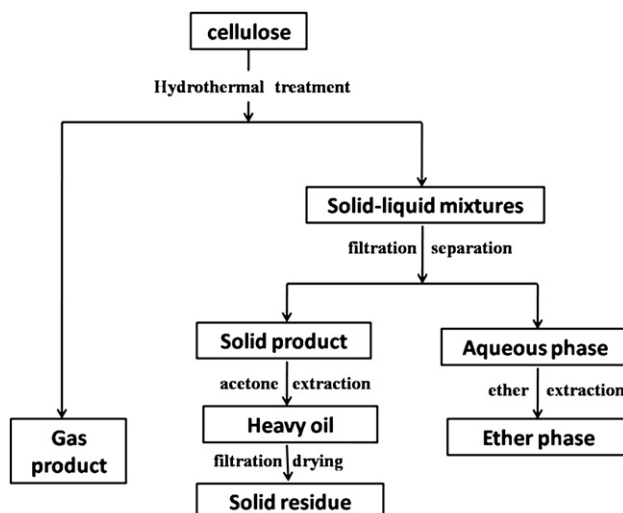


Fig. 2. Products separation after hydrothermal treatment.

2.4. Analysis of liquid

FTIR: The FTIR spectra obtained using a Bruker VERTEX-70 Series in the wave number ranged from 400 cm^{-1} to 4000 cm^{-1} . The aqueous phase was evaporated to completely remove the water before FTIR analysis was conducted. After evaporation, the residues were ground to fine particles and mixed with KBr powder to prepare the pellets for FTIR analysis. The ratio of the sample to KBr powder was kept at about 1:110. The background was subtracted from the sample spectrum.

GC–MS: After ether extraction, the aqueous phase was separated and detected through GC–MS (HP7890 series GC with an HP5975 MS detector equipped with HP-5 chromatographic column). The film in the column was composed of bonded 5% Phenyl and 95% Methyl Siloxane. The GC–MS operating conditions were as follows: $45\text{ }^{\circ}\text{C}$ for 5 min, increased to $250\text{ }^{\circ}\text{C}$ at a rate of $5\text{ }^{\circ}\text{C}/\text{min}$, and finally maintained at $250\text{ }^{\circ}\text{C}$ for 10 min. After acetone extraction, the HO was analyzed by GC–MS using a DB-WAX chromatographic column with a temperature program of $45\text{ }^{\circ}\text{C}$ for 5 min, increased to $280\text{ }^{\circ}\text{C}$ at a rate of $10\text{ }^{\circ}\text{C}/\text{min}$, and finally maintained at $280\text{ }^{\circ}\text{C}$ for 10 min.

2.5. Analysis of solid residues

Elemental analysis: Elemental analyses of the dried solid residues for carbon, hydrogen, and oxygen were carried out with an elementary analyzer (Vario Micro Cube, Germany), and the higher heating value (HHV) was calculated.

SEM/TEM: The solid products were analyzed by scanning electron microscopy (SEM, Quanta200, FEI, Holland) and transmission electron microscopy (TEM, Tecnai G220). The TEM was operated at an acceleration potential of 200 kV. The SRs were prepared for TEM analysis by ultrasonically suspending the powder sample in ethanol and placing a drop of the suspension on a holey carbon copper grid. After evaporation of the solvent, the SRs were introduced into the TEM microscope column.

FTIR/XPS: The chemical composition of the SR was analyzed by FTIR and X-ray photoelectron spectroscopy (XPS, VG Multilab 2000). X-ray photoelectron spectra were obtained with a vacuum generator using MgK α radiation.

TGA: Thermal analysis of SR was carried out in a thermogravimetric analyzer (TGA, NETZSCH STA 409C, Germany). About 10 mg sample SR was placed in a sample pan. The temperature was increased from ambient temperature to $800\text{ }^{\circ}\text{C}$ with a heating rate of $10\text{ }^{\circ}\text{C}/\text{min}$. The TG experiments were performed under flowing purified nitrogen (99.9995%) atmosphere at a flow rate of 100 ml/min.

3. Result and discussion

3.1. Product distribution from cellulose decomposition

Hydrothermal temperature is crucial for the production of HO, gas, and solid residue from cellulose hydrothermal in an autoclave. Research has shown that for most biomass samples, the maximum HO yield is affected by temperature [18]. In the present work, the hydrothermal temperature was varied from $200\text{ }^{\circ}\text{C}$ to $400\text{ }^{\circ}\text{C}$ for 30 min. Results referring to gases, HO, and SR yields were presented to demonstrate the effect of hydrothermal temperature. The product yields were shown as a function of the hydrothermal temperature, as indicated in Fig. 3(a). With the temperature increasing from $200\text{ }^{\circ}\text{C}$ to $250\text{ }^{\circ}\text{C}$, HO yield increased sharply from 5 wt% to 14.75 wt%. A maximum oil yield of 14.75% from $250\text{ }^{\circ}\text{C}$ was the suitable temperature for liquefaction to obtain higher liquid products. Considering the results of other hydrothermal studies, Zhou et al. obtained a maximum bio-oil yield via *Enteromorpha prolifera* hydrothermal of 23.0 wt% at $300\text{ }^{\circ}\text{C}$ with 5 wt% Na_2CO_3 and reaction time of 30 min [19]. Yang et al. obtained HO yield via birch wood hydrothermal liquefaction of 9.8 wt% at $300\text{ }^{\circ}\text{C}$ for 30 min with a stainless steel autoclave [20]. As the temperature exceeded $285\text{ }^{\circ}\text{C}$, the oil yield from cellulose decreased, which is a clear indication that HO from cellulose easily decomposes with increase in temperature. This finding is in agreement with the experimental results of Yu et al. [21]. The reason for the foregoing result is that the oil from cellulose mainly consists of glucose and oligomer, as well as small amounts of ketone, aldehyde, and acid compounds at $240\text{ }^{\circ}\text{C}$ – $270\text{ }^{\circ}\text{C}$. The production of glucose is very sensitive to temperature, and it can be easily decomposed at temperatures over $300\text{ }^{\circ}\text{C}$, while the secondary decomposition of oil to char and gases is occurring.

3.2. Effect of temperature

As indicated in Fig. 3(a), the SR yields decreased as the temperature was increased from $200\text{ }^{\circ}\text{C}$ to $400\text{ }^{\circ}\text{C}$, because the decomposition reaction of cellulose to oligosaccharides occurs at the particle surface of microcrystalline cellulose below $250\text{ }^{\circ}\text{C}$ [22]. Increasing the temperature results in a more complete decomposition of the cellulose by the fragmentation of its molecules into components that result into either liquids or incondensable low-molecular gas.

The influence of temperature on the distribution of gaseous products from hydrothermal cellulose can be found in previous works [23]. The effects of temperature on the gas compositions and yield of the cellulose hydrothermal were also investigated, as

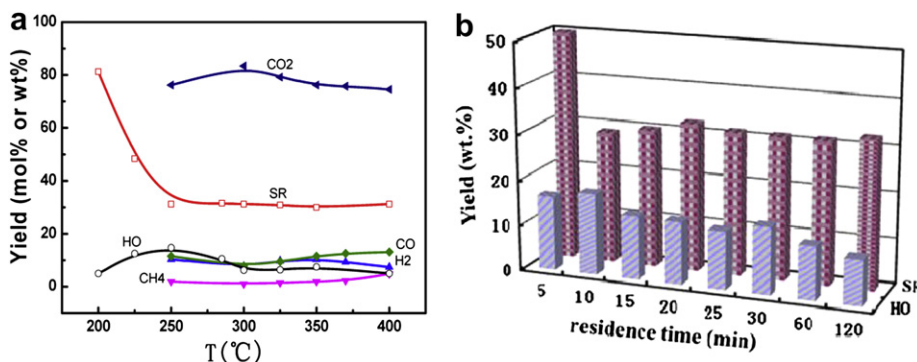
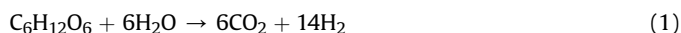


Fig. 3. Product distribution of cellulose (a) Temperature profile of the yields of gases (mol%), SR (wt%), and HO (wt%) for 30 min (b) Time profile of the yields of SR (wt%) and HO (wt%) for $250\text{ }^{\circ}\text{C}$.

indicated in Fig. 3(a). The main gas products were H₂, CO, CO₂, and CH₄. The volume fraction of CO₂ was the highest, and there was a substantial decrease in the CO₂ volume fraction from 83.35% to 74.52% over the hydrothermal temperature range of 300 °C–400 °C. CO₂ was mainly released from the carbonyl (C=O) and COOH. The HO and aqueous phase contained a lot of acids, aldehydes, and ketones. The yield of CO first decreased from 11.53% to 7.79% as the temperature increased to 300 °C. However, it increased to 13.14% as the temperature continuously increased to 400 °C. The yields of CH₄ also increased from 1.92% to 4.89%, whereas that of H₂ content increased to about 10.60% as the temperature increased from 250 °C to 350 °C. With further increase of temperature to 400 °C, the H₂ content decreased significantly to 7.45%. With increasing temperature and pressure, the yield of H₂ decreased, whereas that of CH₄ increased. CH₄, H₂, and CO₂ may also be produced as illustrated by Eqs. (1) and (2) [24].



The above results suggest that the decrease of SR was due to the aggravation of cellulose macromolecular decomposition with the temperature increase. In addition, rising temperature led to the secondary decomposition of the hydrothermal products of cellulose, which could result in the further decomposition of condensable gas products into incondensable low-molecular gas. Thus, the yield of liquid products decreased and incondensable gas products increased. If the hydrothermal reaction is mainly for producing liquid products, the hydrothermal temperature should be controlled at about 250 °C. For hydrothermal gasification, the temperature should be above 350 °C to obtain more gas products.

3.3. Effect of treatment time

An experiment at 250 °C temperature was conducted to study the effect of residence time on the hydrothermal of cellulose. The residence time was varied from 5 min to 2 h. Fig. 3(b) shows the yield (wt%) of HO and SR. At the same temperature with residence time of 5 min, the SR yield reached a maximum of 48.5% and HO yield was 16.25%. Therefore, it can be concluded that shorter residence time improves the hydrolysis of cellulose components into water-soluble products, thus inhibiting further decomposition reaction of cellulose to form HO. With increase in residence time, HO yield increased until 10 min, and thereafter decreased with further increase in the residence time because of the cracking reaction occurring in the primary hydrothermal product of HO. Qu et al. reported maximum HO yield obtained from *Cunninghamia lanceolata* at 320 °C with reaction time of 10 min [25]. Boocock and Sherman found that longer reaction time suppresses oil yield [26]. There was no significant change in the yields of the solid residues from 10 min to 2 h, indicating that longer residence time does not have much influence on the yield of solid residues. The effects of residence time in increasing the dehydration of cellulose and enhancing the formation of organic acid from the hydrolysis reactions formed a small amount of HO.

3.4. Characterization of liquid product

The GC/MS analysis results of HO obtained at 200, 250, 300, 350, and 400 °C with 30 min residence time are shown in Table 2. The chemical compounds identified are mainly furans, phenols, carboxylic acids, aldehydes, ketones, and high molecular compounds. The main compounds at 200 °C were 4-hydroxy-4-methyl-2-pentanone and 5-(hydroxymethyl)-2-furaldehyde (5-HMF), usually used as

drugs and health products to prevent neurodegenerative diseases. The main compounds in HO obtained at 250 °C were levulinic acid (LA) and di-n-octyl phthalate. The ratio of 5-HMF decreased at 250 °C. LA might be formed by the decomposition of 5-HMF with some side reactions during the hydrothermal treatment in the case of cellulose [27]. When the temperature increased to 300 °C, 1,4-benzodioxan-6-carboxaldehyde and benzaldehyde, 2,4,5-trimethyl- were the main compounds. When the reaction temperature increased to 350 °C, the composition of the oil became more complex. Many fused heterocycle, hexa-heterocycle, and five-membered heterocycle compounds were produced as well, such as 1-Acetyl-5-aminoinoline, 1,3,5-trimethyl-1H-Pyrazole, 2,4,5-trimethyl-Benzaldehyde, and 2-Methyl-5-hydroxybenzofuran. The content of the HO obtained at 400 °C was lower than at 350 °C for 30 min. Some major compounds were 2,4,5-trimethyl-benzaldehyde, 2,3-dihydro-1H-Inden-1-one, and cyclopropyl-benzene.

The aqueous phase obtained at 250 °C with 30 min residence time was analyzed by GC/MS and FTIR to study its chemical constituents. The GC/MS results showed that the aqueous phase mainly contained furfural and 5-HMF (Table 3), in agreement with the study of [28]. The aqueous phase included parts of the monosaccharide, so it was insoluble in ether and could not be detected by GC–MS. Therefore, FTIR was employed to analyze the compositions and structural characteristics of the aqueous phase. Fig. 4 shows the following characteristics of the aqueous phase: the IR absorption bands of 3600 cm⁻¹ to 3200 cm⁻¹ resulted from the hydroxyl stretching vibration. The absorbance peak at 3000 cm⁻¹ to 2800 cm⁻¹ represented the C–H stretching vibration of carbohydrate and the absorbance peak at 1400 cm⁻¹ to 1200 cm⁻¹ represented the C–H deformation stretching of carbohydrate. The absorption bands at 1000 cm⁻¹ to 700 cm⁻¹ were the characteristic absorption peaks of β-pyranoside linkage. The results of FTIR showed that the aqueous phase had obvious characteristic peaks on the monosaccharide.

In summary, the composition of the HO became more complex for many high molecular compounds produced at 350 °C. The aldehyde content in the aqueous phase was higher than that in heavy oil at 250 °C and 30 min residence time, showing that the hydrolysis was dominant at 250 °C. The cellulose was hydrolyzed to oligosaccharides and glucose, and then glucose dehydrated to aldehydes at relatively low temperature. With continuous increase in temperature, important intermediate products were produced, such as acids, ketones, aldehydes, and other unknown products through hydrolysis. At the same time, hydrolysis products reacted with each other to form gases, soluble polymers, and black insoluble objects, which affected the quality of the oil and the selectivity of the reactions. The chemical composition and quality of HO were probably determined by the reaction temperature [29–31].

3.5. Characterization of solid residue

3.5.1. Fuel properties of SR (elemental analysis, HHV)

The elemental compositions of the solid residues from the hydrothermal of cellulose at 200 °C–400 °C for 30 min are shown in Table 4. The relationship between the hydrogen/carbon (H/C) and oxygen/carbon (O/C) ratios of the solid residues are also shown in the table. The H/C and O/C ratio decreased continuously with increasing temperature. However, the H/C and O/C ratio decreased initially as the temperature increased to 250 °C but became constant at higher temperatures. These results were consistent with the yield of the gases and solid residues with the same temperature. The elemental analysis of chars was also consistent with the results of the IR analyses. The aromatization probably occurred via condensation, leading to lower H/C ratios after 250 °C. With increase in temperature, the aromatic nature of the solid

Table 2
GC/MS analysis results of the HO products from different temperatures with cellulose for 30 min.

	Name of compound	Molecular formula	Area (%)				
			200 °C	250 °C	300 °C	350 °C	400 °C
Acids	Acetic acid	C ₂ H ₄ O ₂	2.60	3.42	1.57	3.02	1.94
	Levulinic acid	C ₅ H ₈ O ₃	1.26	9.95	3.95	2.62	1.26
	n-Hexadecanoic acid	C ₁₆ H ₃₂ O ₂	1.65	0.9	1.06	–	2.71
Aldehydes	Furfural	C ₅ H ₄ O ₂	1.99	0.67	0.67	–	0.9
	2-Furancarboxaldehyde, 5-methyl-	C ₆ H ₆ O ₂	0.47	0.51	0.71	1.00	0.87
	Benzaldehyde, 2,3,4,5-tetramethyl-	C ₁₁ H ₁₃ O	–	–	1.55	2.58	1.79
	2-Furancarboxaldehyde,5-(hydroxymethyl)-	C ₆ H ₆ O ₃	54.16	4.97	–	–	–
	2,5-Furandicarboxaldehyde	C ₆ H ₄ O ₃	0.57	–	–	–	–
	1,4-Benzodioxan-6-carboxaldehyde	C ₉ H ₈ O ₃	–	–	5.95	–	–
Furan	Benzaldehyde, 2,4,5-trimethyl-	C ₁₀ H ₁₂ O	–	3.71	5.46	8.20	4.02
	2-Acetyl-5-methylfuran	C ₇ H ₈ O ₂	–	0.49	1.39	1.34	1.36
	2-Methyl-5-hydroxybenzofuran	C ₉ H ₈ O ₂	–	3.71	0.96	8.2	1.36
Esters	1,2-Benzenedicarboxylic acid, diisooctyl ester	C ₂₄ H ₃₈ O ₄	–	5.79	–	–	–
	1,2-Benzenedicarboxylic acid, mono(2-ethylhexyl) ester	C ₁₆ H ₂₂ O ₄	–	6	–	–	–
	Di-n-octyl phthalate	C ₂₄ H ₃₈ O ₄	–	16.05	–	–	–
Phenols	Phenol	C ₆ H ₆ O	–	0.68	1.5	3.25	–
	Phenol, 3-methyl-	C ₇ H ₈ O	0.37	0.4	1.4	2.03	2.84
	Phenol, 2,2'-methylenebis[6-(1,1-dimethylethyl)-4-methyl-phenol, 2,4-dimethyl-	C ₂₃ H ₃₂ O ₂	–	5.85	–	10.07	–
Ketones	Phenol, 2,4-dimethyl-	C ₈ H ₁₀ O	–	–	1.11	2.91	1.46
	2-Pentanone, 4-hydroxy-4-methyl-	C ₆ H ₁₂ O ₂	9.56	3.28	3.18	1.78	–
	1H-Inden-1-one, 2,3-dihydro-	C ₉ H ₈ O	–	0.56	1.81	2.59	4.39
	1H-Inden-5-ol, 2,3-dihydro-	C ₉ H ₁₀ O	–	–	–	4.63	3.67
	2-Cyclopenten-1-one, 3-methyl-	C ₆ H ₈ O	–	0.54	1.42	3.1	2.35
	2-Cyclopenten-1-one, 2,3-dimethyl-	C ₇ H ₁₀ O	–	0.27	1.4	3.66	3.58
Phenyl	1,2-Cyclopentanedione, 3-methyl-	C ₆ H ₈ O ₂	0.23	5.26	–	–	–
	Benzene, 1-pentenyl-	C ₁₁ H ₁₄	–	–	1.25	1.77	1.67
	Benzene, cyclopropyl-	C ₉ H ₁₀	–	0.38	3.24	5.42	4.24
Others	1H-Pyrazole, 1,3,5-trimethyl-	C ₆ H ₁₀ N ₂	–	0.92	2.54	4.14	–
	1,6-Anhydro-2,4-dideoxy-.beta.-D-ribo-hexopyranose	C ₆ H ₁₀ O ₃	1.13	–	–	–	–
	1-Naphthalenol, 4-methoxy-	C ₁₁ H ₁₀ O ₂	1.17	1.45	2.32	3.06	–
	Indole, 5-methyl-2-(4-pyridyl)-	C ₁₄ H ₁₂ N ₂	–	–	1.64	–	–
	5,8-Dimethyl-1,2,3,4-tetrahydroquinoxaline	C ₁₀ H ₁₄ N ₂	–	–	–	4	2.44
	1,4-Dimethyl-4,5,7,8-tetrahydroimidazo-[4,5-E]-1,4-diazepin-5,8(6H)-dione	C ₈ H ₁₀ N ₄ O ₂	–	–	3.97	–	–
	1-Acetyl-5-aminindoline	C ₁₀ H ₁₂ N ₂ O	–	0.51	2.65	4.63	–
Total area			75.16	70.27	52.7	84	42.85

residues was higher, and the decreased solid residue yield was accompanied by an increase in the evolution of CH₄. The aromatic hydrocarbons of the side-chain methyl groups and H combined to form CH₄. The O/C ratio decreased after 250 °C because of the possibility of oxygen loss by decarbonylation as the amount of CO₂ and CO was observed. On the other hand, the HHV increased from 15.35 MJ/kg to 26.02 MJ/kg at 400 °C.

3.5.2. Structural characteristics of SR

3.5.2.1. SEM/TEM analysis. The physical and chemical properties of the solid residues were characterized. The SEM images of the cellulose and SR are shown in Fig. 5(a–c). The figures show

Table 3
GC/MS analysis results for the aqueous phase obtained from cellulose at 250 °C and, 30 min residence time.

Chemical compounds	Molecular formula	Area (%)
Furfural	C ₅ H ₄ O ₂	20.84
2-Butanone	C ₄ H ₈ O ₁	2.38
Ethanone, 1-(2-furanyl)-	C ₆ H ₆ O ₂	1.92
2-Furancarboxaldehyde, 5-methyl-	C ₆ H ₆ O ₂	6.90
2-Acetyl-5-methylfuran	C ₇ H ₈ O ₂	1.82
2-Cyclopenten-1-one, 2-hydroxy-3-methyl-	C ₆ H ₈ O ₂	1.85
1,2-Cyclopentanedione, 3-methyl-	C ₆ H ₈ O ₂	2.85
Pentanoic acid, 4-oxo-	C ₅ H ₈ O ₃	3.59
4-Methoxy-4-methyl-2-pentanol	C ₇ H ₁₆ O ₂	3.11
2-Furancarboxaldehyde, 5-(hydroxymethyl)-	C ₆ H ₆ O ₃	11.67
Hydroquinone	C ₆ H ₆ O ₂	1.49
Pyridine, 4-(1-pyrrolidinyl)-	C ₉ H ₁₂ N ₂	1.32
1,4-Benzodioxan-6-carboxaldehyde	C ₉ H ₈ O ₃	3.19

a comparison of the cellulose and its SR obtained from 250 °C at 30 min and 2 h. The surface of the cellulose is shown in Fig. 5(a), but no presence of microspheres, trenches, or surface cracks was visible. After hydrothermal treatment, the original morphology of the sample changed, as can be seen from Fig. 5(b, c). The microspheres and trenches were visible on the surface of the SR, and the microspheres were not evenly distributed. The microspheres were in the growth stage with higher yield and even distribution over

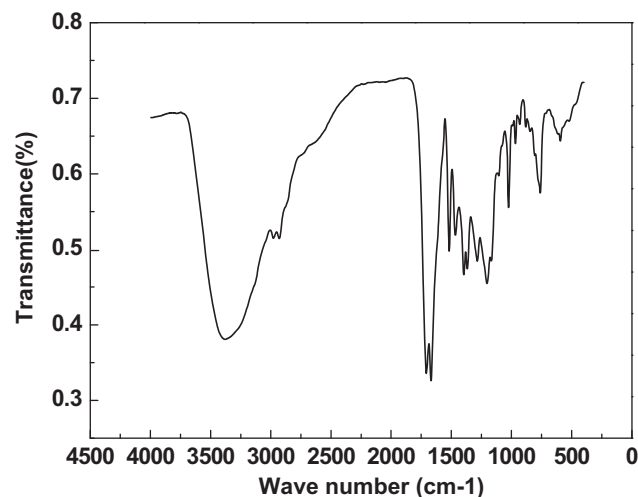


Fig. 4. FTIR spectra of the aqueous phase obtained from cellulose at 250 °C and 30 min residence time.

Table 4
Main characteristics of the solid residues from the different temperatures for 30 min.

Characteristics	Temperature				
	200 °C	250 °C	300 °C	350 °C	400 °C
Elemental analysis ^a (%)					
C	44.54	69.93	71.24	71.48	72.93
H	6.34	4.19	4.12	4.1	3.84
O	49.12	25.91	24.45	24.3	23.14
Empirical formula	CH _{1.71} O _{0.83}	CH _{0.72} O _{0.28}	CH _{0.69} O _{0.26}	CH _{0.69} O _{0.25}	CH _{0.63} O _{0.24}
H/C molar ratio	1.71	0.72	0.7	0.69	0.63
O/C molar ratio	0.83	0.28	0.26	0.25	0.24
HHV ^b	15.35	25.01	25.61	25.69	26.02

^a Weight percentage on dry ash free basis.

^b HHV calculated by the Dulong Formula, $HHV = 0.3383C + 1.422(H-O/8)$.

the surface of SR under residence time of 2 h. The microspheres were about 1 μm in diameter. The carbon spheres varied substantially and systematically with the increase in residence time. According to the SR_{250-2h} TEM analysis (Fig. 5(d)), the microspheres have typical core–shell structure.

3.5.2.2. FTIR analyses. The FTIR spectrum of SR is shown in Fig. 6. Compared with the IR spectrum of cellulose, the intensity of SR decreased during the hydrothermal processing. The bands at 3341 cm^{-1} (–OH) and 1032 cm^{-1} (C–OH) indicated a large amount of hydroxyl groups in the cellulose. The broad absorbance peak of C–H vibration at 2930 cm^{-1} and the C–H deformation vibration at 1460 cm^{-1} indicated the presence of alkanes. The absorbance peak at 2350 cm^{-1} represented the O=C=O stretching vibration,

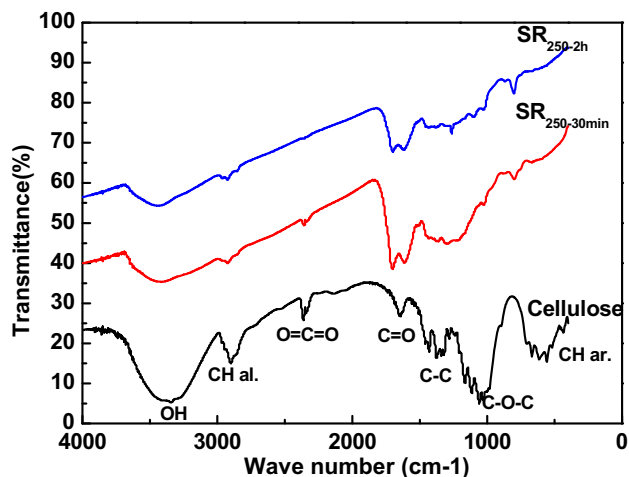


Fig. 6. FTIR spectra of cellulose and solid residues.

indicating CO₂ generation, which was quickly released with the increase of residence time. Therefore, there was no O=C=O adsorption at 250 °C, 2 h. The adsorption of the C=O vibration peak was wider, which indicated the existence of ketones and aldehydes. The band at 1600 cm^{-1} represented aromatic ring skeleton vibrations. The presence of aromatic rings between 900 and 650 cm^{-1} indicated the presence of aromatic esters. The results showed that SR was composed of aromatics and polymeric products.

3.5.2.3. XPS. The XPS spectra of cellulose and SR produced from hydrothermal treatment at 250 °C for 2 h are depicted in Fig. 7(a). The Cls (about 285 eV) and O1s (about 531 eV) peaks were clearly

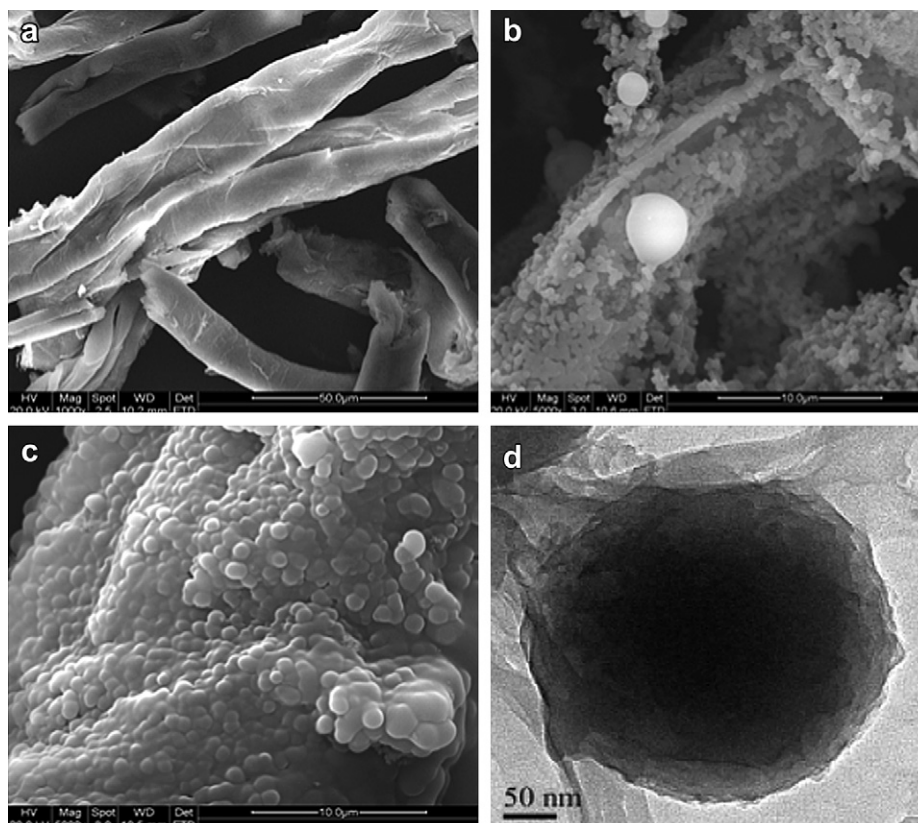


Fig. 5. SEM image of (a) cellulose, (b) SR from 250 °C, 30 min (c) SR from 250 °C, 2 h, and (d) TEM image of SR from 250 °C, 2 h.

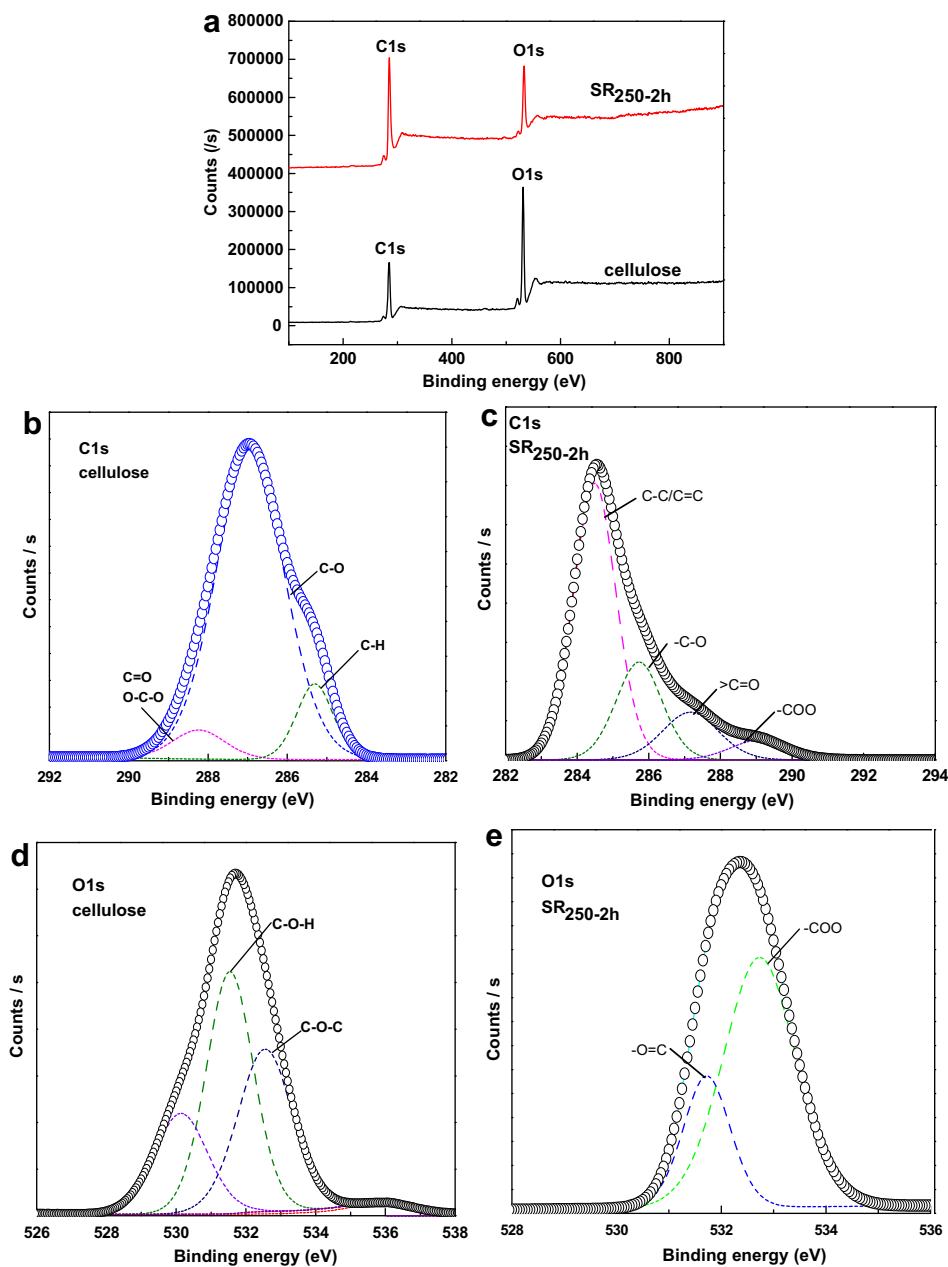


Fig. 7. (a) X-ray photoelectron spectroscopy (XPS) survey spectra of cellulose and SR_{250-2h} (b, c) C1s spectra of cellulose and SR_{250-2h} (d, e) O1s spectra of cellulose and SR_{250-2h}.

resolved. The photoelectron peaks showed that the SR consisted of mainly carbon and oxygen. The intensity of the O1s peak decreased with longer residence time hydrothermal treatment, so the carbon atoms increased against the oxygen atoms. This phenomenon may be attributed to the formation of some condensed aromatic rings.

The C1s and O1s spectra were chosen to investigate the change in the chemical structure of SR. XPS measurement was performed to characterize the functional groups on the sample surface. Cellulose is a macromolecular compound made by glucose molecules linked through β -glycosidic linkages. There is a large amount of hydroxyl group attached to the carbon atom in the cellulose. As shown in Fig. 7(b, c), cellulose exhibited three peaks in XPS C1s spectra attributed to C-O (alcohols and ethers), C=O (acetal), and C-H. The C-O peak was higher than the other functional groups as a whole, which is in very good agreement with the chemical structure of cellulose. Compared with cellulose, the XPS C1s spectra of the SR contained additional aliphatic/aromatic carbon groups (C-C/C=C)

and carboxylic groups, esters, or lactones (-COOR) [32–34]. The results indicated the presence of more oxygen-rich functional groups in the SR surface. FTIR results also verified the presence of these groups on the sample surface.

The XPS O1s results of cellulose and SR are shown in Fig. 7(d, e). In the O1s core-level spectrum of cellulose, the binding energies at 531.5 and 532.5 eV can be assigned to the C-OH and C-O-C groups. The presence of these oxygenated groups was confirmed on the surface of the samples by the O1s spectrum (Fig. 7(d)). Compared with cellulose, the surface of SR has high COO- and low C=O. The corresponding binding energies to peaks of COO- and C=O are 531.7 and 533.0 eV (Sevilla and Fuertes 2009b). The small peaks shift at about 01s; therefore, in the literature, the O1s peaks are rarely discussed.

Compared with the results from the FTIR spectra, the basic behavior of the functional groups of SR_{250-2h} can be investigated by XPS. From the C1s spectra of XPS, the CH, C-O, and C=O groups decreased with increase in residence time, similar to the results

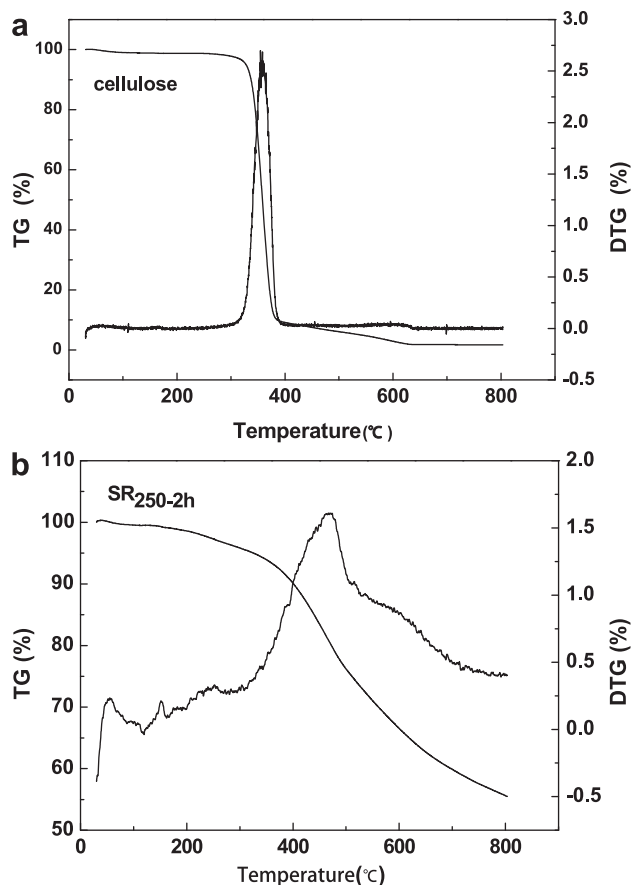


Fig. 8. TG-DTG curves of cellulose and SR_{250-2h}.

obtained with FTIR. Based on the SEM, TEM, FTIR, and XPS results, the SR had a core–shell structure. The core contained ketone and ether groups and the shell contained carboxylic and carbonyl groups. Longer residence time is favorable for the utilization of SR in the fields of new functional carbon materials.

3.5.2.4. Thermal analyses (TG/DTG). The thermogravimetry and derivative thermogravimetry curves of cellulose and SR_{250-2h} are shown in Fig. 8. There was a significant difference in their thermal degradation characteristics. Cellulose was composed of long linear chain-like glucose molecules that were mainly crystalline in structure [35]. Its stable and resistant structure makes cellulose difficult to thermally degrade. The TG/DTG curves of cellulose showed that maximum weight loss occurred in the temperature range 315 °C–400 °C. The residues were about 6.6 wt%. By contrast, nearly 44 wt% of SR_{250-2h} remained at 800 °C. The thermal degradation of SR_{250-2h} showed two major weight loss ranges. The first weight loss step, which included the removal of moisture content and volatile matter, occurred at a temperature range between 50 and 200 °C. The second stage, which consisted of the cracking of organic compounds, occurred at temperature over 200 °C. The results showed that the SR exhibited good thermal stability at high decomposition temperatures.

4. Conclusion

In the present work, cellulose hydrothermal treatment by hot compressed water was carried out in an autoclave at temperature range of 200 °C–400 °C and residence time of 5 min to 2 h. When the hydrothermal reaction is mainly for producing bio-oil, the

temperature should be controlled at about 250 °C for shorter residence time. For gasification, the temperature should be above 350 °C to obtain more gas products. Although the SR did not show a significant change in its yield, the characteristics of the SR continued changing even for longer residence time.

1. The maximum HO and SR yields were 14.75% (250 °C) and 81.25% (200 °C) at the residence time of 30 min, respectively. The gas products mainly consisted of CO₂, CO, CH₄, and H₂ at 250 °C–400 °C. The prolonged residence time did not facilitate the production of oil.
2. HO contained furans, phenols, carboxylic acids, aldehydes, ketones, and high molecular compounds. The aqueous phase contained sugars and its degradation products (aldehydes, phenol, ketones, and acid groups). The HHV of SR produced after 250 °C in just 30 min was comparable to that of bituminous-grade coal. Thus, liquid products can be used as fuel after improvement.
3. Based on the SEM, TEM, FTIR, and XPS results, the SR had a core–shell structure. The core contained ketone and ether groups and the shell contained carboxylic and carbonyl groups. Longer residence time is favorable for the utilization of SR in the fields of new functional carbon materials. Finally, SR exhibited good thermal stability with high decomposition temperatures.

Acknowledgments

The authors wish to express the great appreciation of the financial support from National Nature Science Foundation of China (50930006 and 51021065) and National Technology Support Program (2011BAD15B05-03).

Appendix A

SR_{250-30min}: SR from 250 °C, 30 min.
SR_{250-2h}: SR from 250 °C, 2 h.

References

- [1] Asadullah M, Tomishige K, Fujimoto K. A novel catalytic process for cellulose gasification to synthesis gas. *Catalysis Communications* 2001;2:63–8.
- [2] Richards GN. Glycolaldehyde from pyrolysis of cellulose. *Journal of Analytical and Applied Pyrolysis* 1987;10:251–5.
- [3] Sinağ A, Yumak T, Balci V, Kruse A. Catalytic hydrothermal conversion of cellulose over SnO₂ and ZnO nanoparticle catalysts. *The Journal of Supercritical Fluids* 2011;56:179–85.
- [4] Su S, Li W, Bai Z, Xiang H, Bai J. Effects of ionic catalysis on hydrogen production by the steam gasification of cellulose. *International Journal of Hydrogen Energy* 2010;35:4459–65.
- [5] Xin Z, Watanabe N, Lam E. Improving efficiency of cellulosic fermentation via genetic engineering to create “Smart Plants” for biofuel production. In: Buckeridge MS, Goldman GH, editors. *Routes to cellulosic ethanol*. New York: Springer; 2011. p. 181–97.
- [6] Libra JA, Ro KS, Kammann C, Funke A, Berge ND, Neubauer Y, et al. Hydrothermal carbonization of biomass residuals: a comparative review of the chemistry, processes and applications of wet and dry pyrolysis. *Biofuels* 2011; 2:71–106.
- [7] Peterson AA, Vogel F, Lachance RP, Froling M, Antal JMJ, Tester JW. Thermochemical biofuel production in hydrothermal media: a review of sub- and supercritical water technologies. *Energy and Environmental Science* 2008;1: 32–65.
- [8] Kruse A, Maniam P, Spieler F. Influence of proteins on the hydrothermal gasification and liquefaction of biomass. 2. model compounds. *Industrial and Engineering Chemistry Research* 2007;46:87–96.
- [9] Donovan JM, Molton PM, Demmitt TF. Effect of pressure, temperature, pH, and carbon monoxide on oil yields from cellulose liquefaction. *Fuel* 1981;60: 898–902.
- [10] Minowa T, Zhen F, Ogi T. Cellulose decomposition in hot-compressed water with alkali or nickel catalyst. *The Journal of Supercritical Fluids* 1998;13: 253–9.

- [11] Minowa T, Fang Z, Ogi T, Varhegyi G. Liquefaction of cellulose in hot compressed water using sodium carbonate: products distribution at different reaction temperatures. *Journal of Chemical Engineering of Japan* 1997;30:186–90.
- [12] Minowa T, Kondo T, Sudirjo ST. Thermochemical liquefaction of Indonesia biomass residues. *Biomass Bioenergy* 1998;14:517–24.
- [13] Xu C, Lad N. Production of heavy oils with high calorific values by direct liquefaction of woody biomass in sub/near-critical water. *Energy Fuels* 2008;22:635–42.
- [14] Elliott DC, Sealock LJ, Butner RS. Product analysis from direct liquefaction of several high-moisture biomass feedstocks. *Pyrolysis Oils from Biomass*. American Chemical Society 1988;376:179–88.
- [15] Zhang B, Keitz MV, Valentas K. Maximizing the liquid fuel yield in a bio-refining process. *Biotechnology and Bioengineering* 2008;101:903–12.
- [16] Toor SS, Rosendahl L, Rudolf A. Hydrothermal liquefaction of biomass: a review of subcritical water technologies. *Energy* 2011;36:2328–42.
- [17] Sevilla M, Fuertes AB. The production of carbon materials by hydrothermal carbonization of cellulose. *Carbon* 2009;47:2281–9.
- [18] Akhtar J, Amin NAS. A review on process conditions for optimum bio-oil yield in hydrothermal liquefaction of biomass. *Renewable and Sustainable Energy Reviews* 2011;15:1615–24.
- [19] Zhou D, Zhang L, Zhang S, Fu H, Chen J. Hydrothermal liquefaction of macroalgae *Enteromorpha prolifera* to bio-oil. *Energy and Fuels* 2010;24:4054–61.
- [20] Yang Y, Gilbert A, Xu C. Production of bio-crude from forestry waste by hydro-liquefaction in sub-/super-critical methanol. *AIChE Journal* 2009;55:807–19.
- [21] Yu Y, Lou X, Wu H. Some recent advances in hydrolysis of biomass in hot-compressed water and its comparisons with other hydrolysis methods. *Energy and Fuels* 2007;22:46–60.
- [22] Kamio E, Sato H, Takahashi S, Noda H, Fukuhara C, Okamura T. Liquefaction kinetics of cellulose treated by hot compressed water under variable temperature conditions. *Journal of Materials Science* 2008;43:2179–88.
- [23] Demirbas A. Hydrogen production from biomass via supercritical water gasification. *Energy Sources, Part A: Recovery, Utilization, and Environmental Effects* 2010;32:1342–54.
- [24] Kruse A, Henningsen T, Sinağ A, Pfeiffer J. Biomass gasification in supercritical water: influence of the dry matter content and the formation of phenols. *Industrial and Engineering Chemistry Research* 2003;42:3711–7.
- [25] Qu Y, Wei X, Zhong C. Experimental study on the direct liquefaction of *Cunninghamia lanceolata* in water. *Energy* 2003;28:597–606.
- [26] Boocock DGB, Sherman KM. Further aspects of powdered poplar wood liquefaction by aqueous pyrolysis. *The Canadian Journal of Chemical Engineering* 1985;63:627–33.
- [27] Horvat J, Klaić B, Metelko B, Sunjic V. Mechanism of levulinic acid formation. *Tetrahedron Letters* 1985;26:2111–4.
- [28] Kamio E, Takahashi S, Noda H, Fukuhara C, Okamura T. Effect of heating rate on liquefaction of cellulose by hot compressed water. *Chemical Engineering Journal* 2008;137:328–38.
- [29] Kabyemela BM, Adschiri T, Malaluan RM, Arai K. Glucose and fructose decomposition in subcritical and supercritical water: detailed reaction pathway, mechanisms, and kinetics. *Industrial and Engineering Chemistry Research* 1999;38:2888–95.
- [30] Karagöz S, Bhaskar T, Muto A, Sakata Y, Oshiki T, Kishimoto T. Low-temperature hydrothermal treatment of biomass: effect of reaction parameters on products and boiling point distributions. *Energy and Fuels* 2004;18:234–41.
- [31] Saeman JF. Kinetics of wood saccharification - hydrolysis of cellulose and decomposition of sugars in dilute acid at high temperature. *Industrial and Engineering Chemistry* 1945;37:43–52.
- [32] Belgacem MN, Czeremuszkin G, Sapieha S, Gandini A. Surface characterization of cellulose fibres by XPS and inverse gas chromatography. *Cellulose* 1995;2:145–57.
- [33] Okpalugo TIT, Papakonstantinou P, Murphy H, McLaughlin J, Brown NMD. High resolution XPS characterization of chemical functionalised MWCNTs and SWCNTs. *Carbon* 2005;43:153–61.
- [34] Xia W, Wang Y, Bergsträsser R, Kundu S, Muhler M. Surface characterization of oxygen-functionalized multi-walled carbon nanotubes by high-resolution X-ray photoelectron spectroscopy and temperature-programmed desorption. *Applied Surface Science* 2007;254:247–50.
- [35] Kumar S, Gupta RB. Hydrolysis of microcrystalline cellulose in subcritical and supercritical water in a continuous flow reactor. *Industrial and Engineering Chemistry Research* 2008;47:9321–9.